#3929

No. 3027

APPLICATION OF NUMERICAL SIMULATION FOR RESIDENTIAL ROOM AIR CONDITIONING

K. Yamazaki **M. Komatsu** **M. Otsubo**
ASHRAE Member

INTRODUCTION

In recent years, there has been an increasing demand for better quality of the air-conditioned environment in residential rooms. If we can estimate such environmental conditions as the airflow and temperature distribution, it becomes easier to select suitable air conditioners or to design air-conditioning systems.

For this purpose, a computational simulation method was developed that can be applied to the conditions in rooms where there are forced convection fields and three-dimensional velocity and temperature distributions.

The flow field generated by an air conditioner can be characterized by a buoyancy force and weak turbulent flow. The equations for conservation of mass, momentum, and energy for an incompressible fluid comprise the basic expressions. A two-equation turbulent model forming the k-ε equations of Launder and Spalding, together with the SIMPLE algorithm of Spalding, was applied to our simulation program. The air temperature from the outlet of the air conditioner is higher or lower than the space air temperature. The buoyancy force of the airflow from an air conditioner has a very important role in air temperature and flow distribution, so this force was analyzed in particular detail.
Many works have been published in this field, but many of them are for two-dimensional computation about natural convection and forced convection with no buoyancy force. Such simulations as our work for real air-conditioned rooms and equipment design are not currently being developed.

In this paper, we have attempted to estimate the air-heating environment for a console type of air heater installed in a residential room and an air diffuser installed on the ceiling.

COMPUTATIONAL METHOD

Basic Equations

Taking the orthogonal coordinate system, we normalized the variables by using the outlet velocity, Uo, as in Equation 1, u, v and w being the velocities respectively in the x, y and z directions, L the characteristic length of the system, and Ta the local average temperature around the point (x,y,z). ν is the kinetic viscosity and ν_t is the turbulent viscosity, ΔT is the temperature difference between the outlet air and wall surface, and the Symbol (*) denotes real values. With the normalized variables, parameters contained in the basic equations were grouped into the Reynolds number (Re), Grashof number (Gr) and Prandtl number (Pr) (Gupta and Srinivasan 1978; Shimoji 1984). The equations of mass, momentum and energy conservation for incompressible fluids are written as Equations 2 through 4 in Table 1, e_i being the unit vector along the z axis and the subscripts varying as i,j = 1,2,3. The k-ε model of Launder and Spalding is written as Equations 5 through 8 in Table 1; k is the turbulent kinetic energy per unit mass, G the rate of its generation, and ε the rate of its dissipation.

K. Yamazaki, M. Komatsu and M. Otsubo, Mitsubishi Electric Corp., Consumer Products Research Lab., 2-14-40 Ofuna, Kamakura 247, JAPAN.

Constants C_1, C_2, and C_μ are given in Launder and Spalding (1974). For the assumed pressure field p* and the corresponding velocity field v*, the pressure correction equation of Patankar and Spalding (Patankar and Spalding 1972; Patankar 1980) was derived by using a simplified relationship between the variations of velocity v' and pressure p'.
The simplification can be written as Equation 9 in Table 1. The pressure correction p' was determined so that the velocity field composed of v* and v' would satisfy the mass conservation. The equation is expressed as Equation 10 in Table 1. Solutions to Equations 2 through 7 and 10 with appropriate boundary conditions gave the desired prediction of the velocity and temperature distribution of the airflow.

Models for Buoyancy Force

The presence of a buoyancy force caused occasional divergence from the iterative process in our computation. We tested several different models for the buoyancy force, and typical results are described here. In accordance with the Bousinesq approximation, the natural model is given by the difference between the temperature of a control volume or cell and that above it. Denoting the term by S, this was expressed by the discretization equation as in Equation 11 in Table 2. However, this led to divergence of the iteration.

The next model took the temperatures on the lower faces only in order to relieve the situation as in Equation 12 in Table 2. This provided convergence, but the temperature distribution obtained was somewhat different from the experimental values. The third and most successful model, shown in Equation 13 in Table 2, includes a term that expresses the fact that the force acts when the mass of a volume of air is lighter than that in front of it, as well as the effects from the upper and lower cells. We took a = 0.2, b = 0.5 and c = 0.3, this expression giving acceptable temperature distributions.

Computer System

Numerical results of the basic fluid mechanics equation groups were obtained by means of the SIMPLE algorithm, and the buoyancy of the airflow from air conditioners was analyzed in particular detail.
In accordance with the shape and dimensions of the appliance and the space to be air-conditioned, data were divided into an irregularly spaced lattice and computation then performed.

These computations were performed by a FORTRAN program on a super-high-speed computer, while transmission of the computational commands and data was executed by a personal computer linked to public telephone lines.

The input data for boundary conditions are expressed as the dimensionless temperature of internal wall surface, which was normalized for the difference between the outlet and wall temperature, and the dimensionless length expressing the room dimensions, which was normalized by the characteristic length of the room.

Data were output as the numerical temperature and airflow from points within an irregularly spaced lattice, the temperature and airflow patterns being displayed on a computer CRT and plotted out.

Flow Chart

According to the foregoing basic equations, the velocity, pressure and temperature were computed by using the SIMPLE algorithm (Patankar 1980), the method being explained by the flow chart in Figure 1. The symbols used are pressure, P; airflow velocity, U; turbulent kinetic energy, k; dissipation rate for turbulent kinetic energy, ε; turbulent viscosity, ν_t; and air temperature, T.

In this program, initialization of the matrix calculation was performed after treating the input data. In the next step, the pressure was assumed before repetition, and by using this assumed pressure, the airflow velocity was calculated and then the pressure.

A velocity-correction was applied from this pressure, before the turbulent kinetic energy and its dissipation rate were calculated from the turbulence model to provide easy convergence.

In the next step, using k and ε, the turbulent viscosity was calculated, followed by the

temperatures from the U and ν_t values as the last stage of repetition. The corrected value that resulted was then judged for convergence and, if unsuitable, a new, corrected pressure was used in place of the first-assumed pressure with a return to the first step of the velocity calculation.

This procedure was repeated until a convergent solution was obtained, the results of these characteristics for the air-conditioned environment being displayed and/or printed out.

EXPERIMENT

Figure 2(a) shows the main components of our experimental system to measure the temperature distribution in a model room. Figure 2(b) shows the model room dimensions and the measuring points for the air temperature distribution.

The model room was built within an environmental test room in which the temperature and humidity were controlled by computer. The dimensions of the room were 3.6 m (L) by 3.6 m (D) by 2.4 m (H), which are identical to those used in the computation, except that the length in the y direction was twice as long as that in the computations.

Recently in Japan, small kerosene or gas air heaters, which have a heating capacity of 2000 kcal/h to 3000 kcal/h, are currently used as domestic room air heaters. This type of air heater was used in our examination and calculation example. The maximum temperature of the air discharged from this air heater was 80°C, but the high-temperature air discharged was restricted to a very small area and most of the occupied space was not influenced by it.

A test sample of an air conditioner was installed in the model room and run until a stable state was reached. The temperature distribution was measured by a sliding lattice with 132 thermocouples attached, which could traverse in steps from end to end in the room. Measured data were recorded and analyzed by a desk-top computer. Figures 3(a) and 3(b) show the measured temperature distributions of the central zone when a console type of air heater was installed in the model room.

Figure 3(a) shows that warm air was blown out horizontally from an outlet in the upper part of the air heater's front panel and drawn into an inlet in its lower part. The warm air temperature at the outlet was about 50°C and air velocity about 3 m/s.

After running horizontally for about 1 meter in front of the air heater, the warm air ascended by its buoyancy force. The temperature in the upper half of the room was heated, but the lower half near the floor remained at a comparatively low temperature. In such a case, a large temperature difference exists between heights corresponding to the head and feet, which is not good for thermal comfort.

Figure 3(b) shows that warm air was blown horizontally from an outlet placed in the lower part of the air heater, and circulated air was drawn into an inlet placed in its upper part. The warm air temperature and velocity were the same as those in Figure 3(a). In this case, warm air ran horizontally above the floor before and after ascent, providing a better temperature distribution in the model room than that in the first case and offering relatively good thermal comfort.

RESULTS OF COMPUTATION

The domain for computation is shown in Figures 4 through 10, and because of the symmetry of the problem, half of the room on one side of the centerline was considered.

In Figures 5 through 8, air heaters are installed on the floor against the west-side wall, air being discharged and drawn in at the center of the front panel of the air heater so that the airflow pattern was symmetrical about the centerline, as shown Figure 4. In this figure the domain for computation is the slashed area. The boundary conditions on the plane through this centerline are given as free-slip conditions for all parameters such as temperatures, velocities, k and ε. The other boundary conditions are given as the temperature of each wall surface, air velocity at the outlet of the air heater, and nonslip conditions on the wall.

The room air space was divided into control volumes by grid lines so that the wall surface was also divided by these lines. We defined the non-uniform boundary conditions of the temperatures, air velocities, k and ε on each control volume surface contacting with the boundary wall. By considering these control volumes, we could calculate for an irregularly

shaped rectangular wall and for inlets and outlets spaced anywhere along the walls.

The boundary conditions imposed were as follows: at the outlet, values of u = Uo, k = Ko and $\varepsilon = \varepsilon o$; and at the inlet, u = Ui, k = Ki, $\varepsilon = \varepsilon i$.
On another portion of the surface and for the remaining surfaces, nonslip conditions for the velocity and the natural boundary condition for k and ε were imposed. To compare the analytical results with experimental data, experimental values are given for the temperature distribution. A natural boundary condition was imposed on the pressure on all the surfaces.

Reynolds numbers used in the calculation of Figure 5 through Figure 10 ranged from 4.6×10^5 to 5.6×10^5. In these calculations, Reynolds number is defined by $Re = L \times U/\nu$, where L is the characteristic length of the room size, U is the outlet air velocity, and ν is the kinetic viscosity. The air heaters provided an outlet air velocity ranging from 2 to 5 m/s.

Figures 5 and 6 show distributions of the airflow and temperature obtained from computation to compare with the experimental results. The difference between the outlet air and wall surface temperature was taken to be 30 deg C, and the outlet air temperature was set at about 50°C. The outlet air velocity was 3.0 m/s, and the flow rate 3.0 m^3/min, corresponding to a Grashof number, $Gr = 1.22 \times 10^{11}$ and $Gr/Re^2 = 0.390$
The turbulent kinetic energy and its dissipation were 0.150×10^{-1} and 0.184×10^{-2}, respectively, at the outlet for the calculation of Figure 5, the value for the other calculation examples being of the same order as that in Figure 5.

These computational conditions are respectively the same as the measured conditions shown in Figures 3(a) and 3(b). In these figures, it can be seen that the main flow was ascending with increasing distance along the x axis. The flow field developed successively and gradually in the whole domain. The temperature distribution shown in Figure 6 has an ascending pattern compared with the measured result shown in Figure 3(b), but these computational temperature distributions generally agree with the respective measured results.

Calculation results are shown by two-dimensional isothermal lines and airflow vectors. When we exactly examine the three-dimensional flow pattern, it is necessary to select many plane views. We show another plane of the airflow pattern in Figure 6. For example, the X-Y plane and Y-Z plane are shown in Figure 7.

Figure 8 shows an example of the computational results for a temperature difference between the outlet air and wall surface of 20°C, the other conditions being the same as those in Figure 6. From the isothermal temperature distribution pattern, the temperature was small compared with the forward one, so that the buoyancy force did not have much influence on the ascending characteristics of the flow flux, with the flow flux extending along the floor.

Figures 9 and 10 show examples of the computed results for the airflow discharging from a diffuser installed in the ceiling. The temperature difference between the outlet air and wall was 30 deg C and the airflow velocity at the outlet was 2.0 m/s. In Figure 9, the warm air discharge point is on one side of the ceiling, and an inlet is installed on the other side of the ceiling. In Figure 10, the outlet position and conditions are same as those in Figure 9, but the inlet is positioned low on an opposite wall. In Figure 9, it is evident that the air from the outlet flows down to the floor and that the main flow flux is curved going up towards the inlet, the temperature distribution appearing to be higher on one side of the outlet and lower on the other side. In Figure 10, the air from the outlet flows downward and runs along the floor before being drawn into the inlet in the lower part of the opposite wall.

The calculated results can be effectively used to determine the basic design for air-conditioning systems, such as the selection of capacity, the outlet and inlet positions in the room, the discharged air volume, velocity, flow direction and temperature, and to estimate the thermal comfort of an air-conditioned room. In these calculations, the air temperature and flow distribution patterns are very important to judge whether or not a zone of discomfort exists.

The explanation has been concerned with air heating, but it is easy to calculate the effect for air cooling by reversing the sign of the buoyancy force.

CONCLUSION

The three-dimensional distribution of airflow and temperature in an air-conditioned room was computed, and the computed temperature distribution of the air was compared with experimental data. Some differences between the computed and experimental results can be attributed to the

coarseness of the grid spacing used and to the interpolation routine for display. Thus, it is reasonable to apply the computational system developed here for practical use in the design and estimation of various air-conditioned room environments.

Further, this computational system can be applied to develop (1) advanced and complex flow patterns to control the ascent of warm air and to generate a comfortable heating environment, (2) air-conditioning systems for semi-open rooms, (3) large buildings with great interior spaces for public use, (4) moving vehicles where various accelerating forces act, and (5) room environments where an experimental investigation is too difficult or expensive to perform.

To better meet the requirements, it is necessary to further save computational time. Our next investigation is being directed toward thermal comfort evaluation and designing comfortable air-conditioned environments.

REFERENCES

Gupta, V., and Srinivasan, J, 1978, "Heat and mass transfer," McGraw-Hill Publishing Co. Ltd.

Launder, B.E., and Spalding, D.B., 1974, "The numerical computation of turbulent flow," Computer Methods in Applied Mechanics and engineering, vol. 3, pp. 269-289.

Patankar, S.V., and Spalding, D.B., 1972, "A calculation procedure for heat, mass and momentum transfer in three-dimensional parabolic flows," Int. J. Heat Mass Transfer, vol. 15, pp. 1787-1806.

Patankar, S.V., 1980, "Numerical heat transfer and fluid flow," McGraw-Hill Book Company.

Simoji, S., 1984, "A comparison of calculation methods of thermally induced flow fields for small personal computers," Proc. 14th Int. Sym. Space Technology and Science, Tokyo.

Sugawara, S., Hara, M., and Yamazaki, K, "Dynamic analysis of indoor temperature distribution," The 4th Int. Sym. on the Use of Computers for Environmental Engineering Related to Buildings.

TABLE 1

Basic Equations and k - ε Equations

$$x=x^*/L,\ y=y^*/L,\ z=z^*/L,\ u=u^*/U_0,\ v=v^*/U_0,\ w=w^*/U_0$$
$$\nu=\nu^*/U_0L,\ \nu_t=\nu_t^*/U_0L,\ T=(T^*-T_a^*)/\Delta T^* \qquad (1)$$

$$\frac{\partial u_j}{\partial x_j} = 0 \qquad (2)$$

$$\frac{\partial}{\partial x_j}(u_iu_j) = -\frac{\partial p}{\partial x_i} + \frac{\partial}{\partial x_j}\left(\frac{1}{Re} + \nu_t\right)\frac{\partial u_i}{\partial x_j} + \frac{\partial}{\partial x_j}\left(\frac{1}{Re} + \nu_t\right)\frac{\partial u_j}{\partial x_i} + e_i\cdot\frac{Gr}{Re^2}\cdot T \qquad (3)$$

$$\frac{\partial}{\partial x_j}(u_jT) = \frac{\partial}{\partial x_j}\left(\frac{1}{Pr\cdot Re} + \frac{\nu_t}{\sigma_T}\right)\frac{\partial T}{\partial x_j} \qquad (4)$$

$$\frac{\partial}{\partial x_j}(u_jk) = \frac{\partial}{\partial x_j}\left(\frac{1}{Re} + \frac{\nu_t}{\sigma_k}\right)\frac{\partial k}{\partial x_j} + G - \varepsilon \qquad (5)$$

$$\frac{\partial}{\partial x_j}(u_j\varepsilon) = \frac{\partial}{\partial x_j}\left(\frac{1}{Re} + \frac{\nu_t}{\sigma_\varepsilon}\right)\frac{\partial \varepsilon}{\partial x_j} + \left(c_1G - c_2\varepsilon\right)\cdot\frac{\varepsilon}{k} \qquad (6)$$

$$G = \nu_t\left(\frac{\partial u_i}{\partial x_j} + \frac{\partial u_j}{\partial x_i}\right)\frac{\partial u_i}{\partial x_j} \qquad (7)$$

$$\nu_t = c_\mu\frac{k^2}{\varepsilon} \qquad (8)$$

$$u_i' = -A(x)\frac{\partial p'}{\partial x_i} \qquad (9)$$

$$\frac{\partial}{\partial x_j}\left(A(x)\frac{\partial p'}{\partial x_j}\right) = \frac{\partial u_j^*}{\partial x_j} \qquad (10)$$

TABLE 2

Model of Buoyance Force

$$S = Gr\ (\ -T(i,j,k+2) + T(i,j,k)\ )/2/Re^2 \qquad (11)$$

$$S = Gr\ (\ -T(i,j,k+1) + T(i,j,k)\ )/Re^2 \qquad (12)$$

$$S = Gr\ (\ -a\,T(i,j,k+1) - b\,T(i,j,k-1) - c\,T(i+1,j,k) + T(i,j,k)\ )/Re^2 \qquad (13)$$

where

$$a + b + c = 1$$

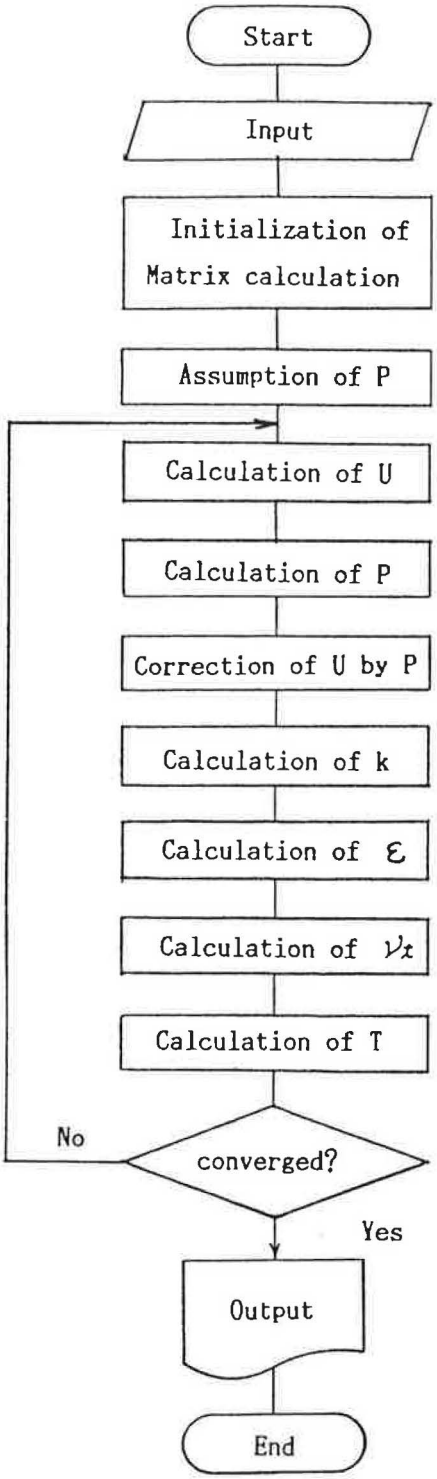

Figure 1. General flow chart of program

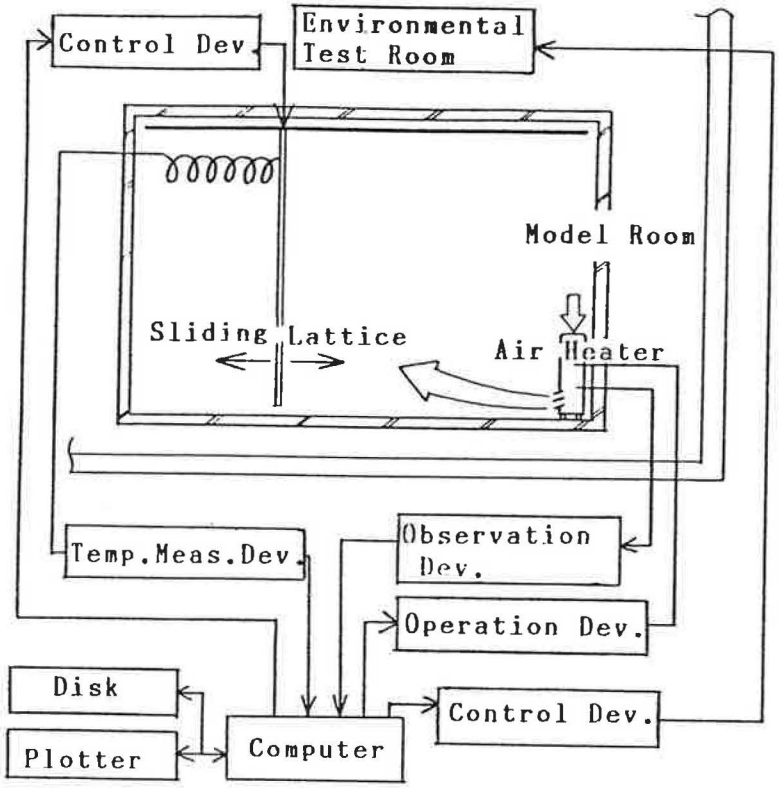

(a) Measuring system

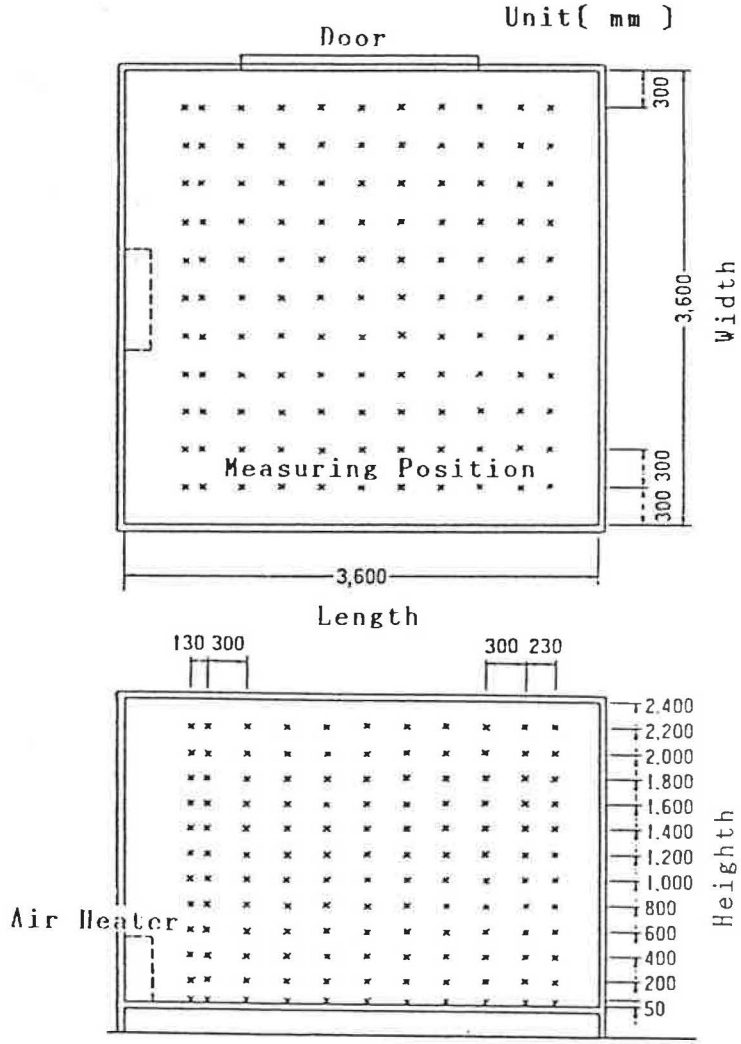

(b) Model room and measuring position of temperatures

Figure 2. Experimental system

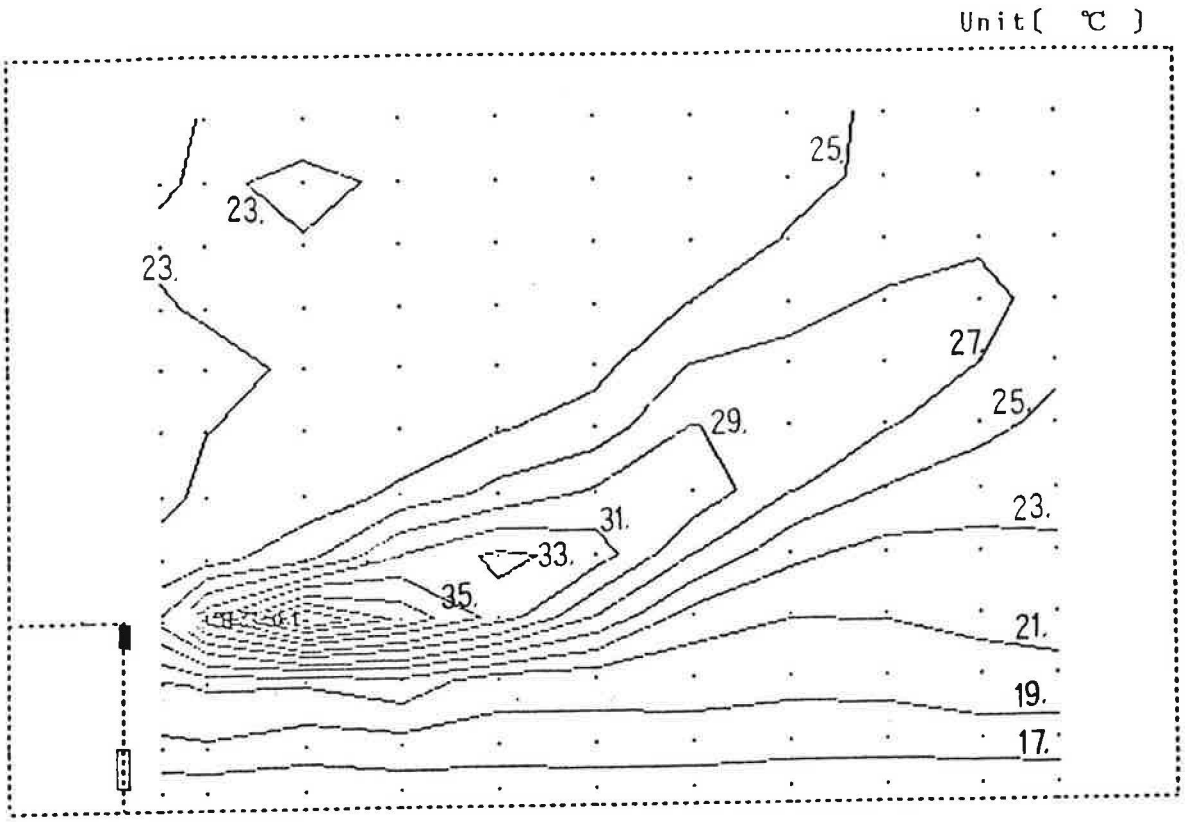

(a) Outlet placed in upper part

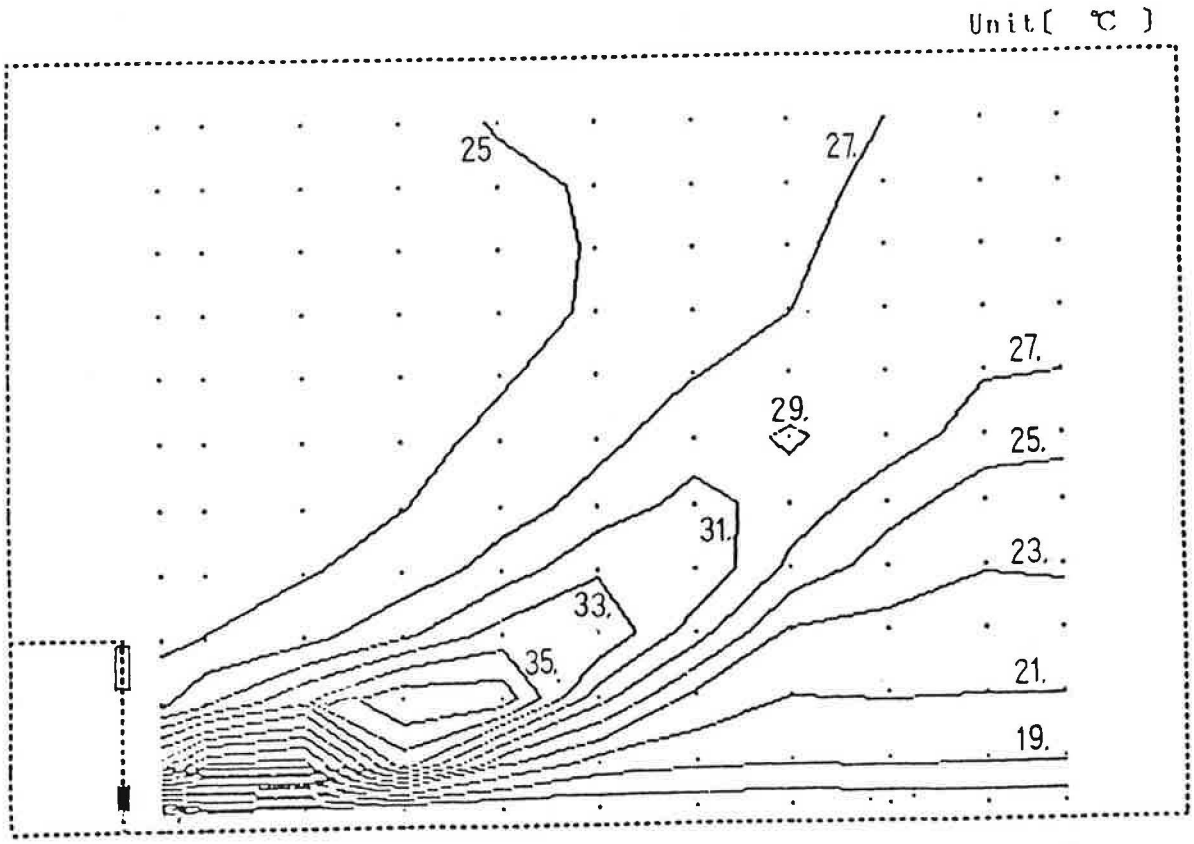

(b) Outlet placed in lower part

Figure 3. Measuring temperature distribution for a console type of air heater

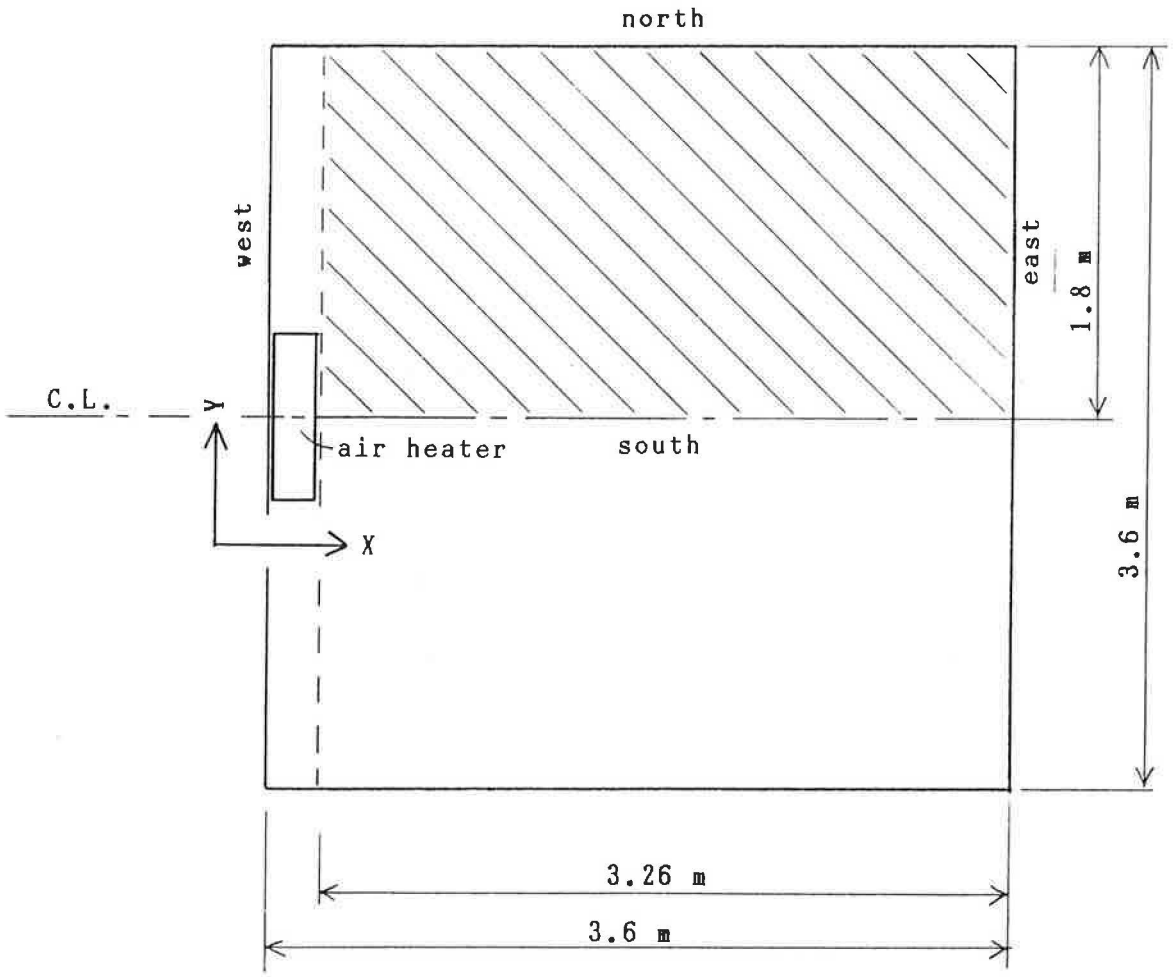

Figure 4. Domain for computation (slashed area)

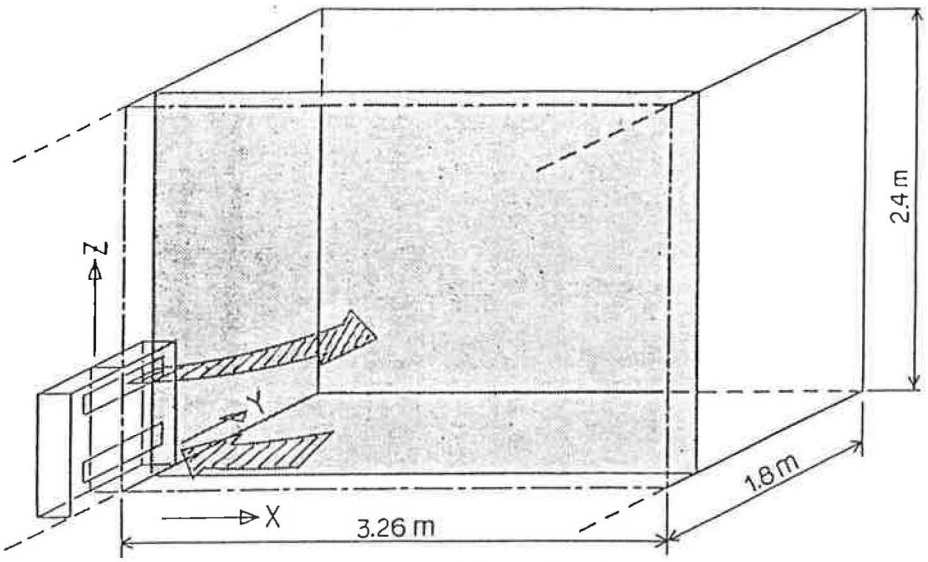

(a) Cut plane

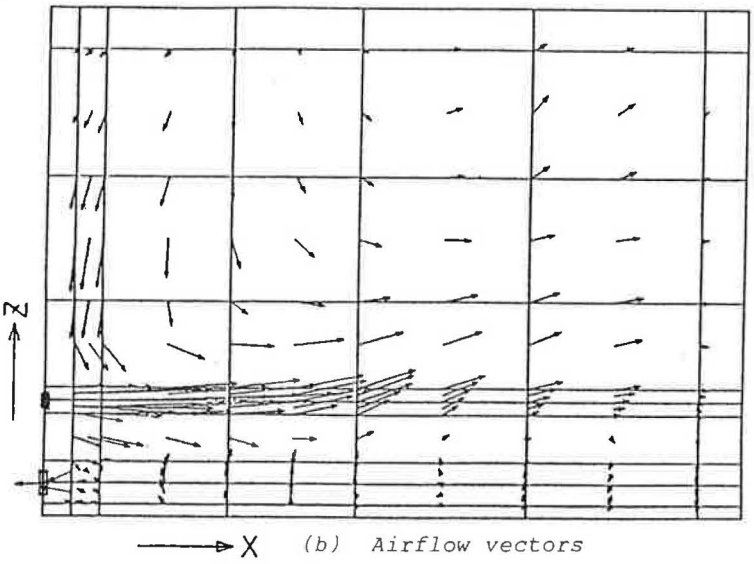

(b) Airflow vectors

Unit(℃)

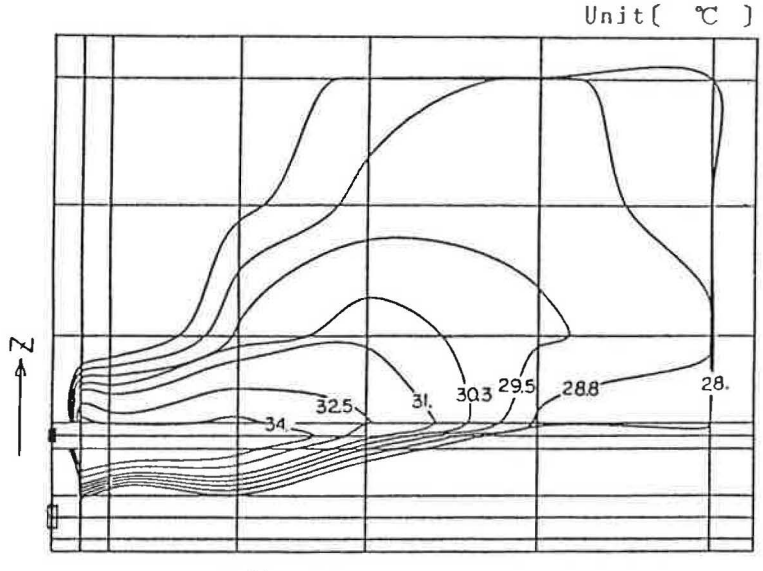

(c) Isothermal lines

Figure 5. Computational airflow and temperature distribution for a console type of air heater (1)

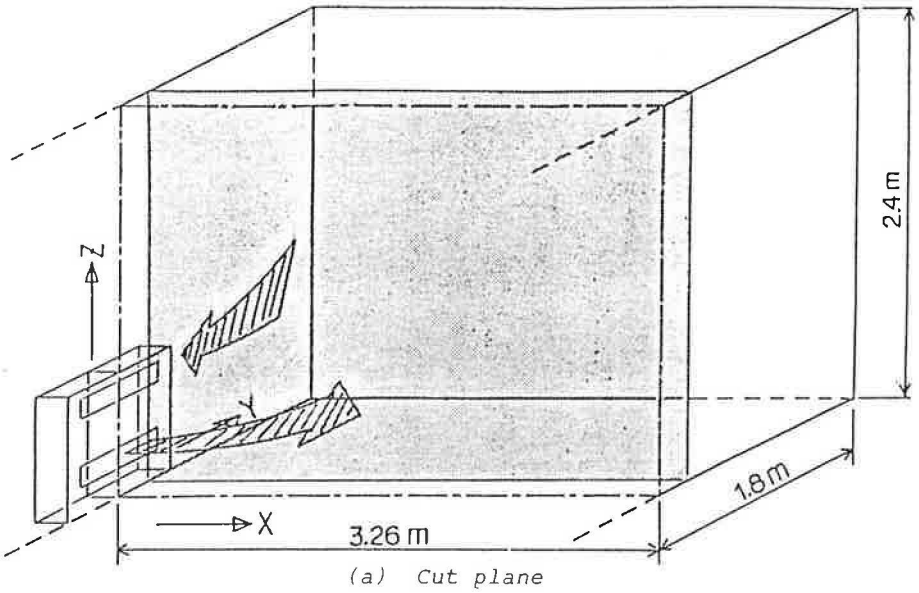

(a) Cut plane

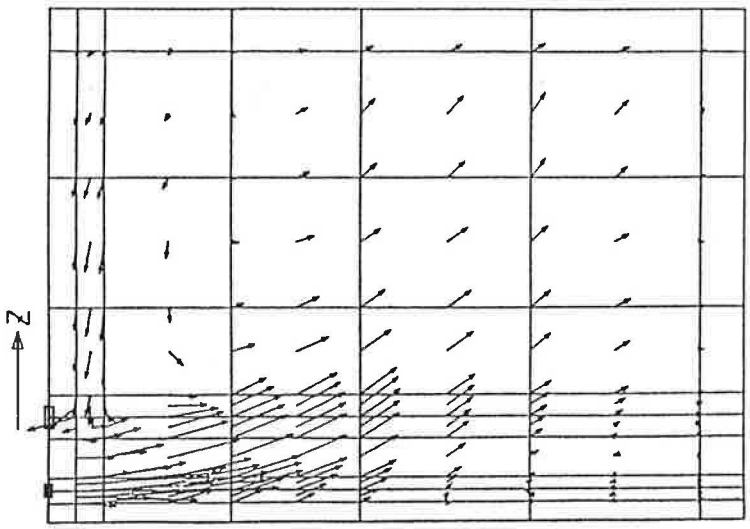

(b) Airflow vectors

Unit[℃]

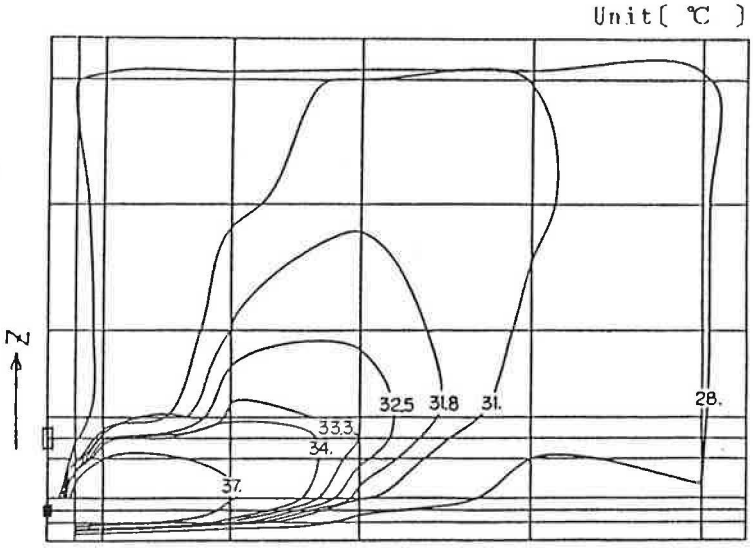

(c) Isothermal lines

Figure 6. Computational airflow and temperature distribution for a console type of air heater (2)

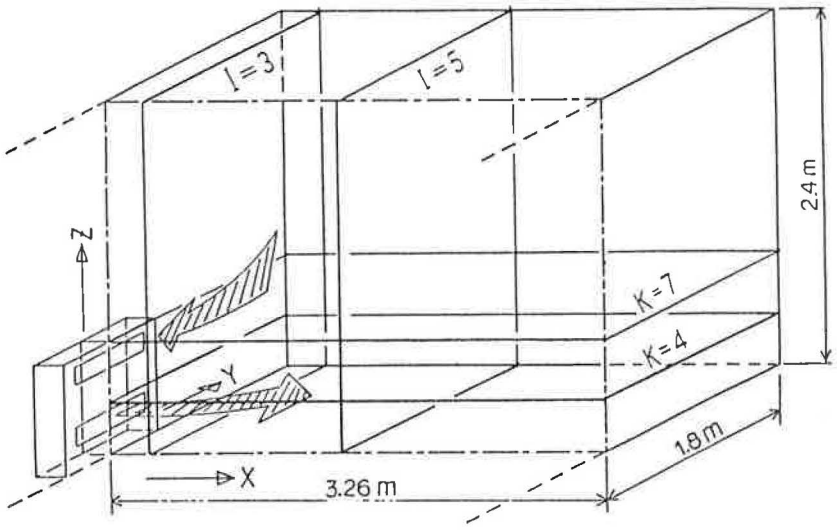

(a) Cut plane

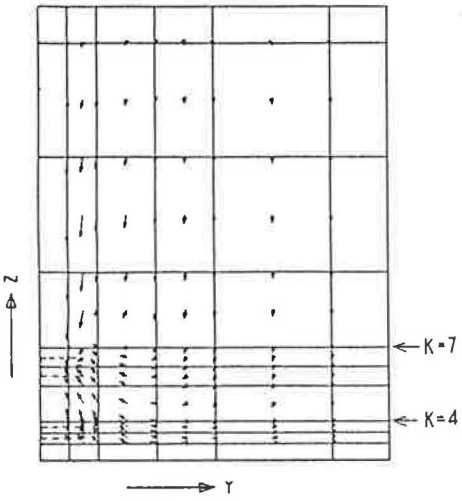

(b) Airflow vector for vertical plane
I = 3

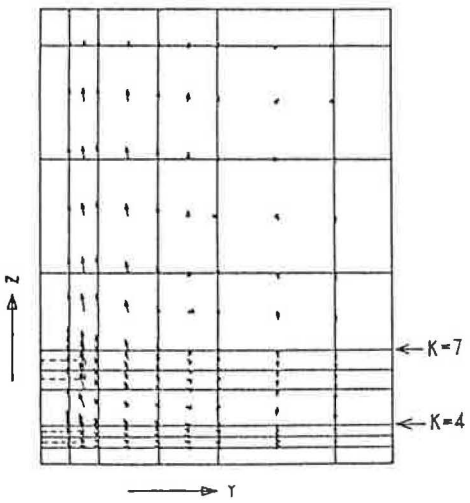

(c) Airflow vector for vertical plane
I = 5

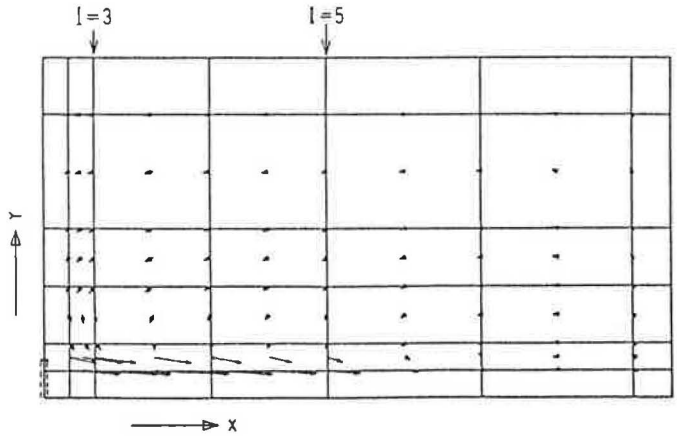

(d) Airflow vector for horizontal plane
K = 4

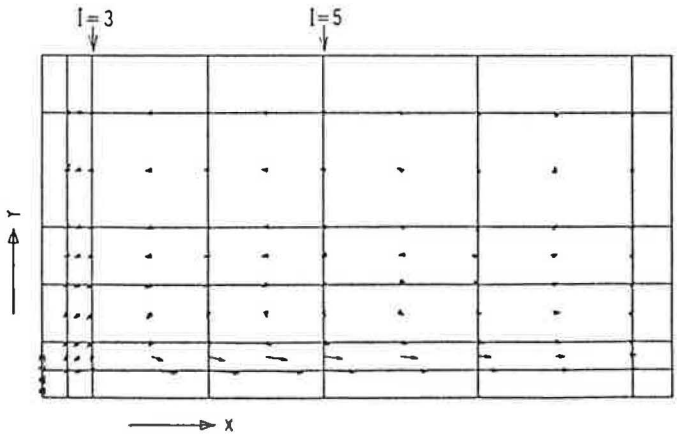

(e) Airflow vector for horizontal plane
K = 7

Figure 7. Computational airflow distribution for a console type of air heater (2)

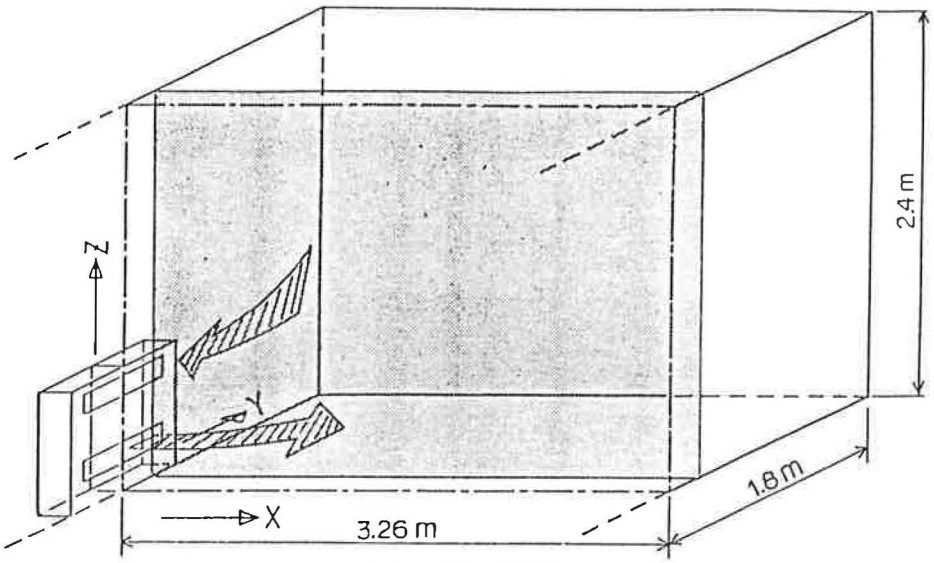

(a) Cut plane

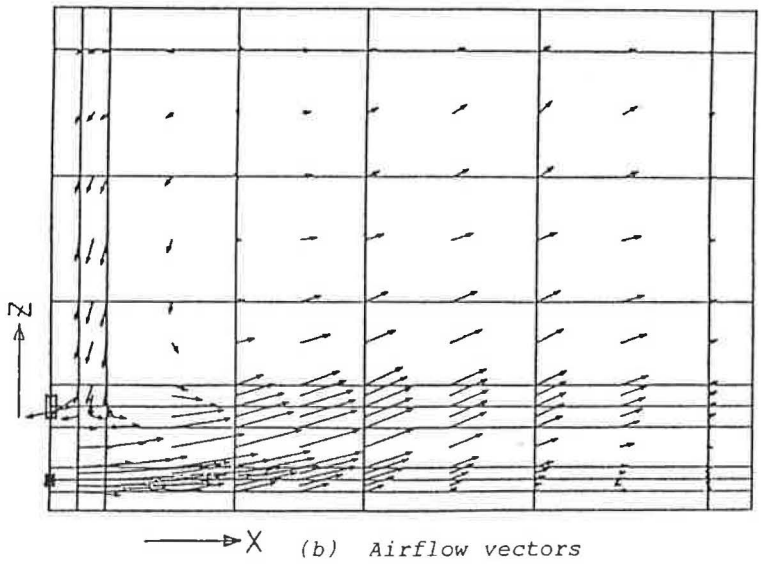

(b) Airflow vectors

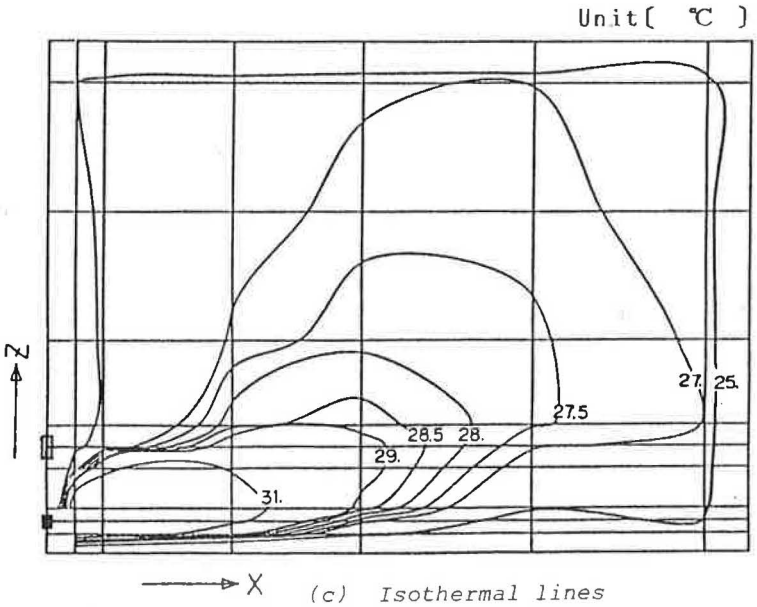

(c) Isothermal lines

Figure 8. Computational airflow and temperature distribution for a console type of air heater (3)

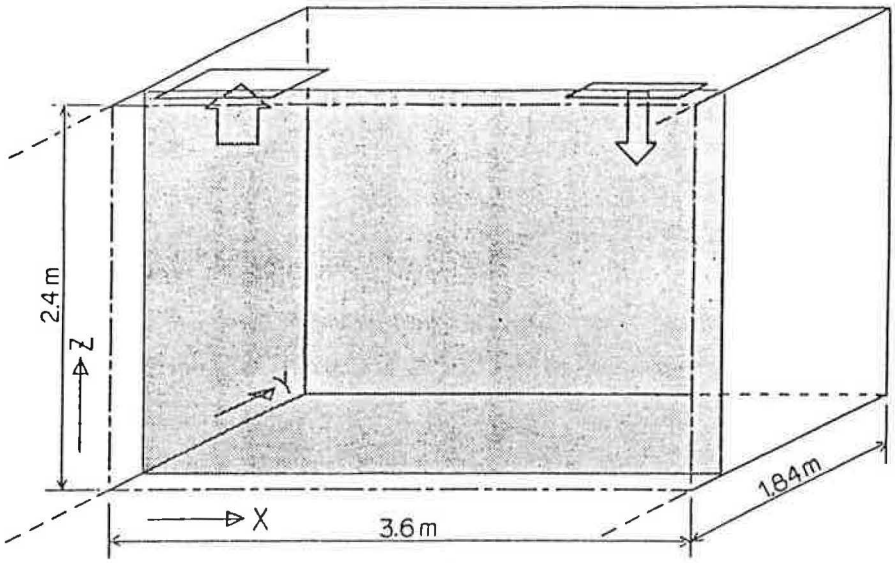

(a) Cut plane

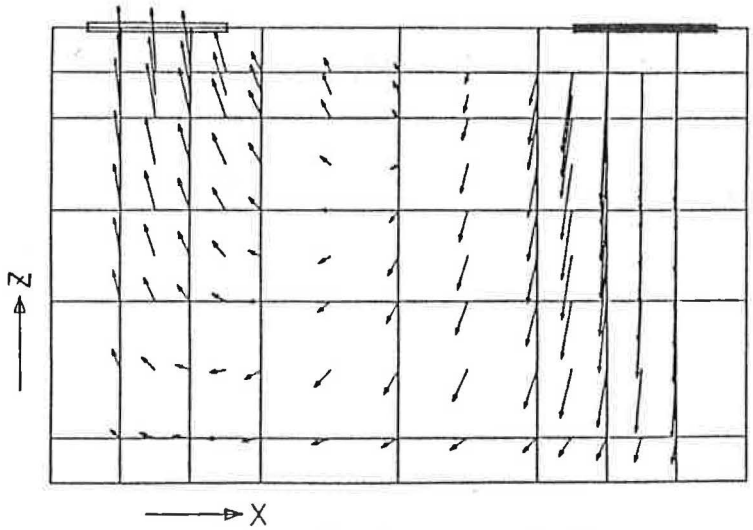

(b) Airflow vectors

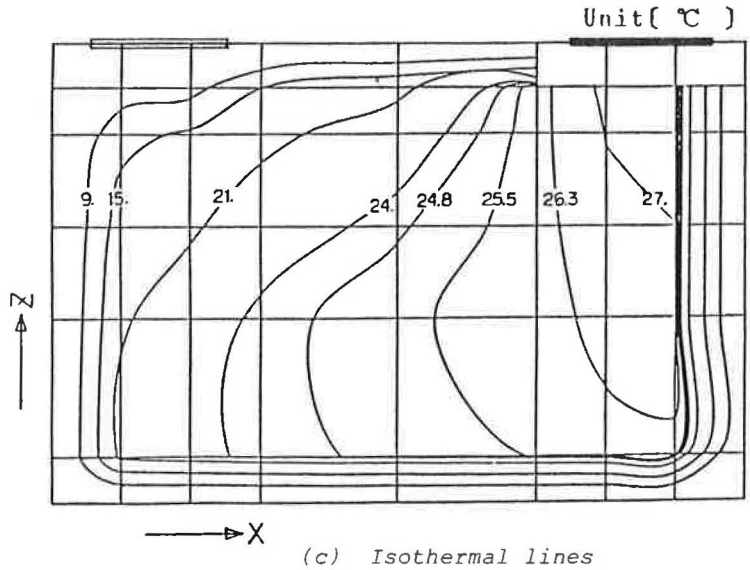

(c) Isothermal lines

Figure 9. Computational airflow and temperature distribution for a ceiling diffuser (1)

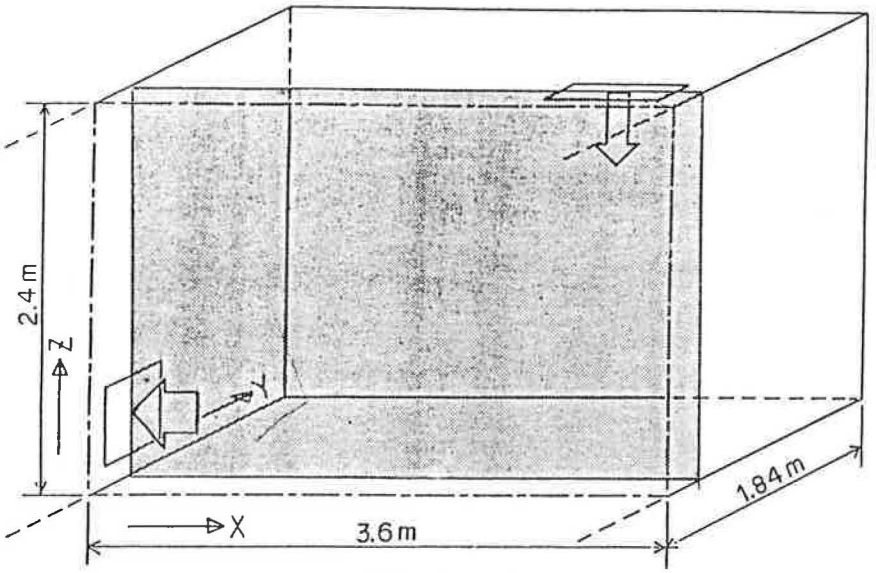

(a) Cut plane

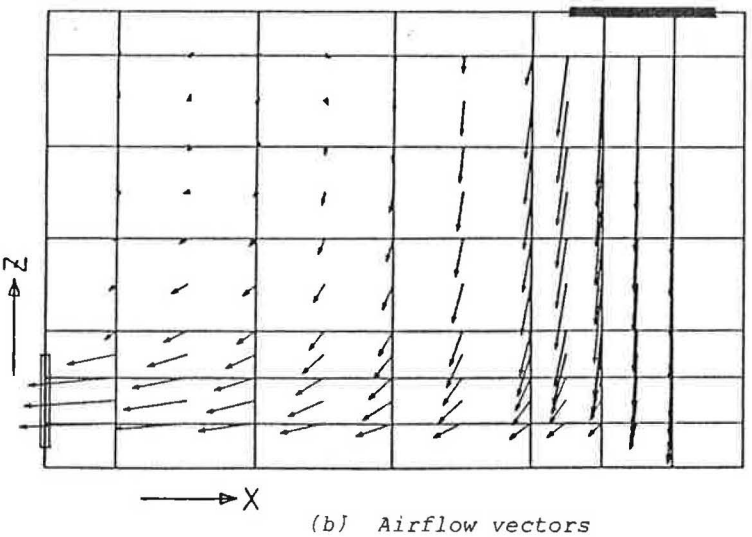

(b) Airflow vectors

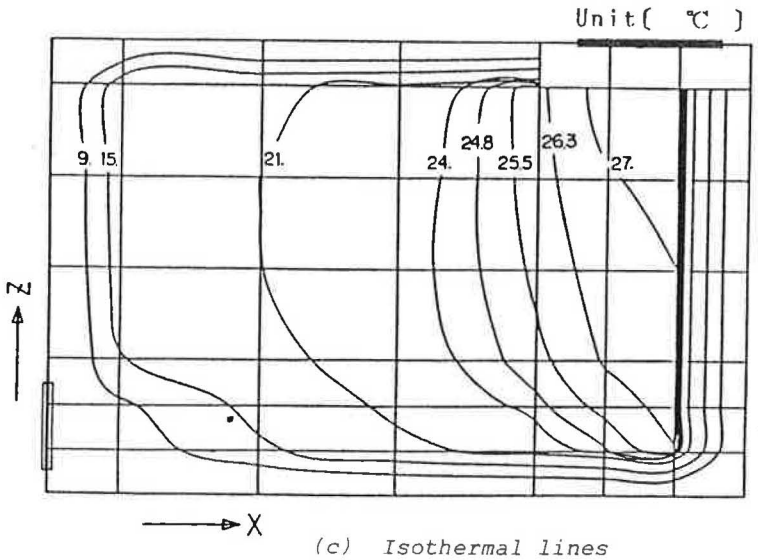

(c) Isothermal lines

Figure 10. Computational airflow and temperature distribution for a ceiling diffuser (2)